Near-Infrared Imager and Slitless Spectrograph/Fine Guidance Sensor (NIRISS/FGS)

MANE 6962 – Space Instrumentation

By : Melissa Flores

Credit: esawebb

Brief Overview: James Webb Telescope

- Launched Dec. 25 2021
- Four Instruments on board
  - Near Infrared Imager and Slitless Spectrograph (FGS/NIRISS)
- First cold space-based IR interferometer
- Suited for finding and characterizing (proto)planets and using transit spectroscopy to study an exoplanets atmosphere
  - Proto-Planet: a large mass currently in orbit and is going through the developmental stages of becoming a planet
  - Transit Spectroscopy: a technique used for exoplanets atmospheres by assessing the change in starlight as it passes by a star
- Demonstrate a binary point source at a 50:1 contrast while exercising dithering
  - To characterize exoplanetary systems and binary star systems
  - Dithering: the intentional, small, random shifts in the telescope's pointing direction between exposures (mas)

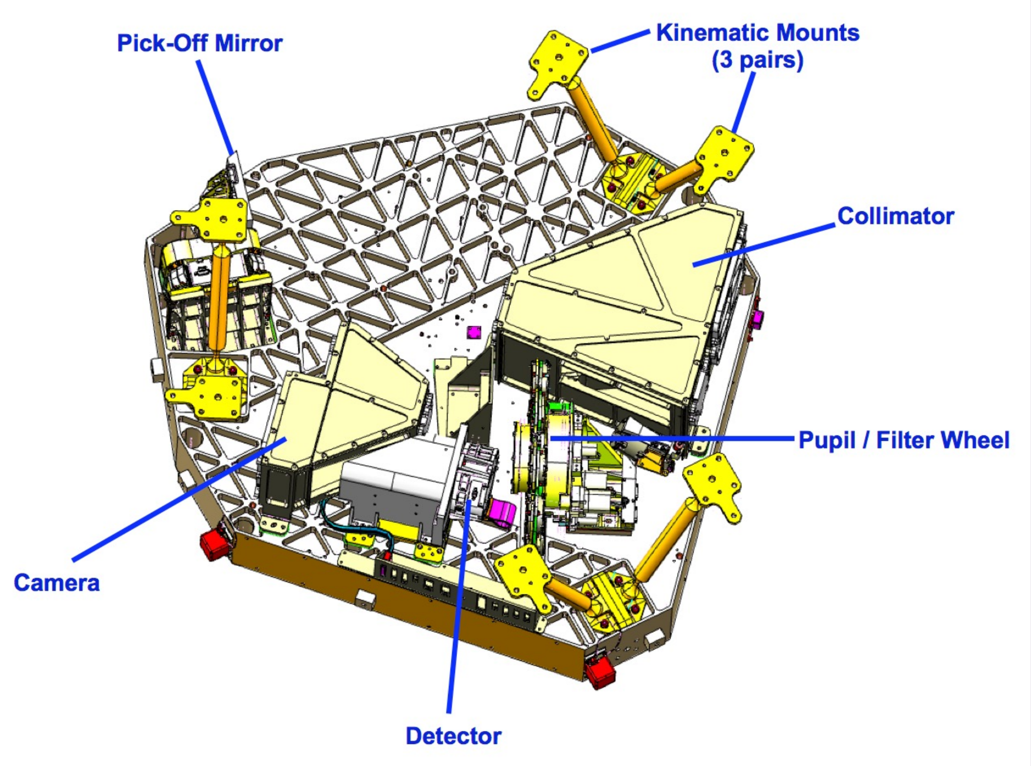

Credit: [Rene et al. 2023]

General Overview of the NIRISS

4 Modes:

- Single Object Slitless Spectroscopy (SOSS)
  - Collects the spectrum of the atmosphere
- Wide Field Slitless Spectroscopy (WFSS)
  - Obtains the spectra of galaxies for analysis
- Aperture Masking Interferometry (AMI)
  - Uses interferometry to distinguish two points of light in an image
- NIRISS Imaging
  - A backup to the Near-Infrared Camera, takes extra near-infrared images

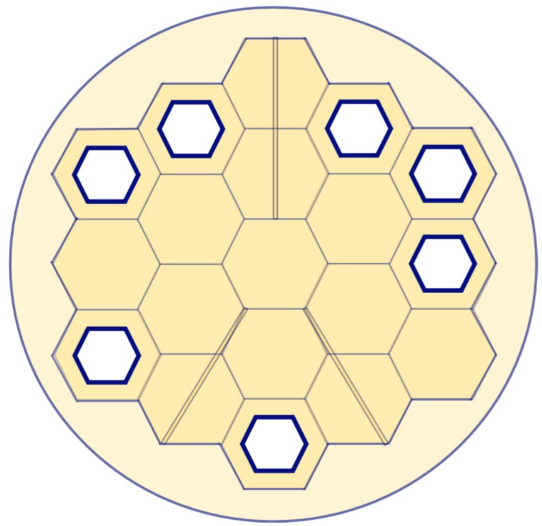

Figure 1. Schematic diagram of the non-redundant mask onboard *JWST*/NIRISS containing seven sub-apertures.

Credit: Ray et al. 2025

Why can’t it be Collected from the Ground?

- Better performance in Closure phase precision and contrast sensitivity by an order of magnitude than current ground telescopes
- More stable than ground optical systems (no atmospheric instabilities) and accurate Closure Phases
- Captures High Contrast Images—to detect faint companions next to bright stars
- Creates interferometric fringes—to collect metrology from the star, and find off axis companions
- “NIRISS AMI will attain contrasts of 8-9 mag at separations ≤100-200 mas between 3 and 5 µm” [8]
    - Enabling precise photometry at longer wavelengths and increasing detection on companions close to a bright source

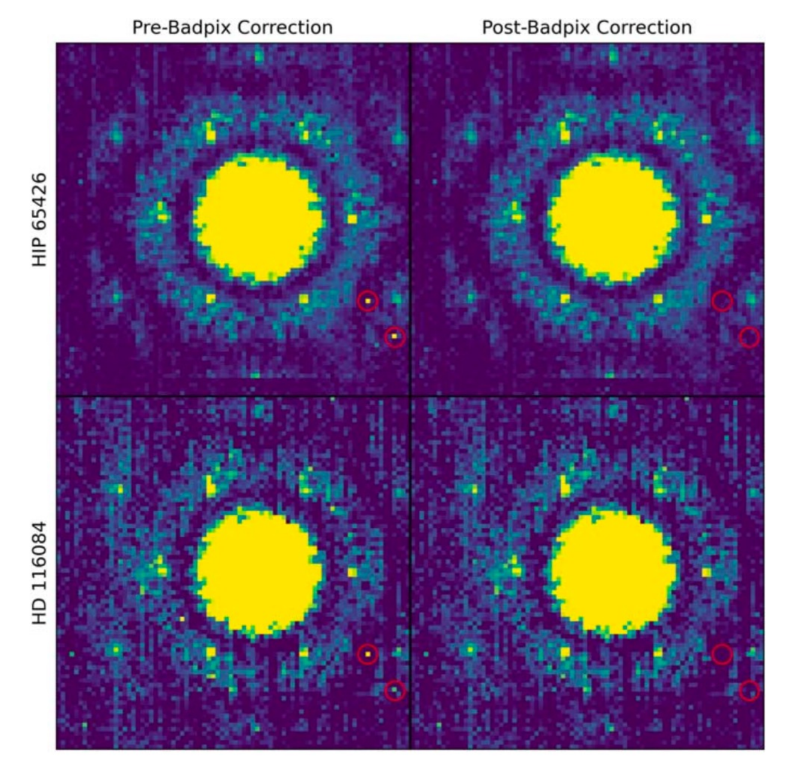

Credit: Sallum et al. 2024

Physical Phenomenon

- Interference from multiple apertures
  - Splits what is taken by the telescope by the seven apertures
  - This will create the fringes that are analyzed
- Apodization of Point Spread Function (PSF)
  - A Super Gaussian Window is applied to the PSF in order to suppress any noisy measurements (reducing any detector related noise)
- Closure Phases determine how faint of a companion you can see
  - There is a disadvantage on the ground due to the atmosphere introducing rapidly varying phase errors which increase the closure phase—limiting the achievable contrast
  - In space the closure phases and the contrast limits are more stable and deeper due to the atmospheric effects being absent

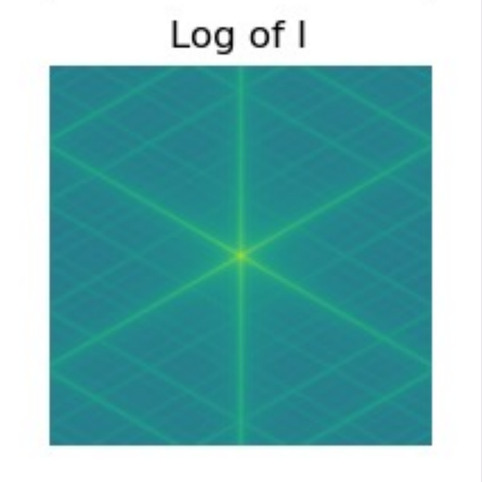

Existing Models

- JWST AMI has GitHub repositories with modeling information for the apertures
  - SAMpy - https://github.com/JWST-ERS1386-AMI/SAMpy/tree/main/SAMpy
    - AMI observations and system performance
  - AMICAL - https://github.com/SAIL-Labs/AMICAL
    - AMI data reduction and model fitting
- Mikulski Archive for Space Telescopes
  - MAST
    - AMI data observations
- JWST Exposure Time Calculator
  - ETC
    - Simulates S/N performance

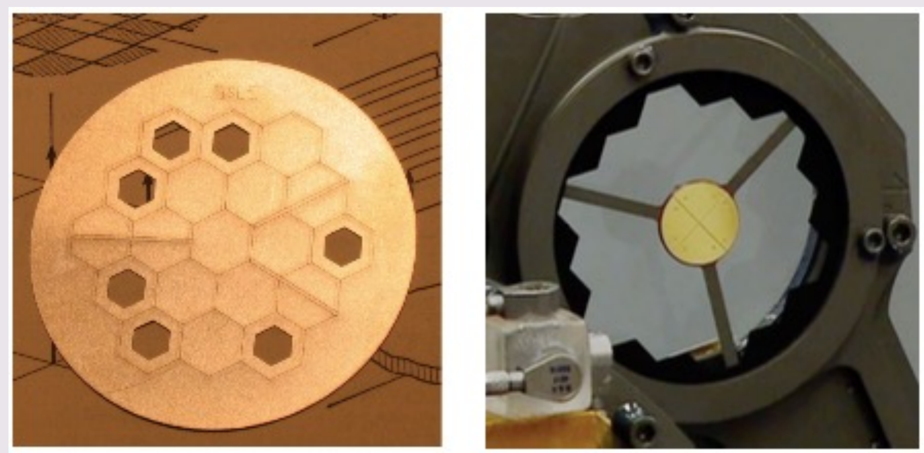

Credit: Sivaramakrishnan et al. 2023

1st Order Results

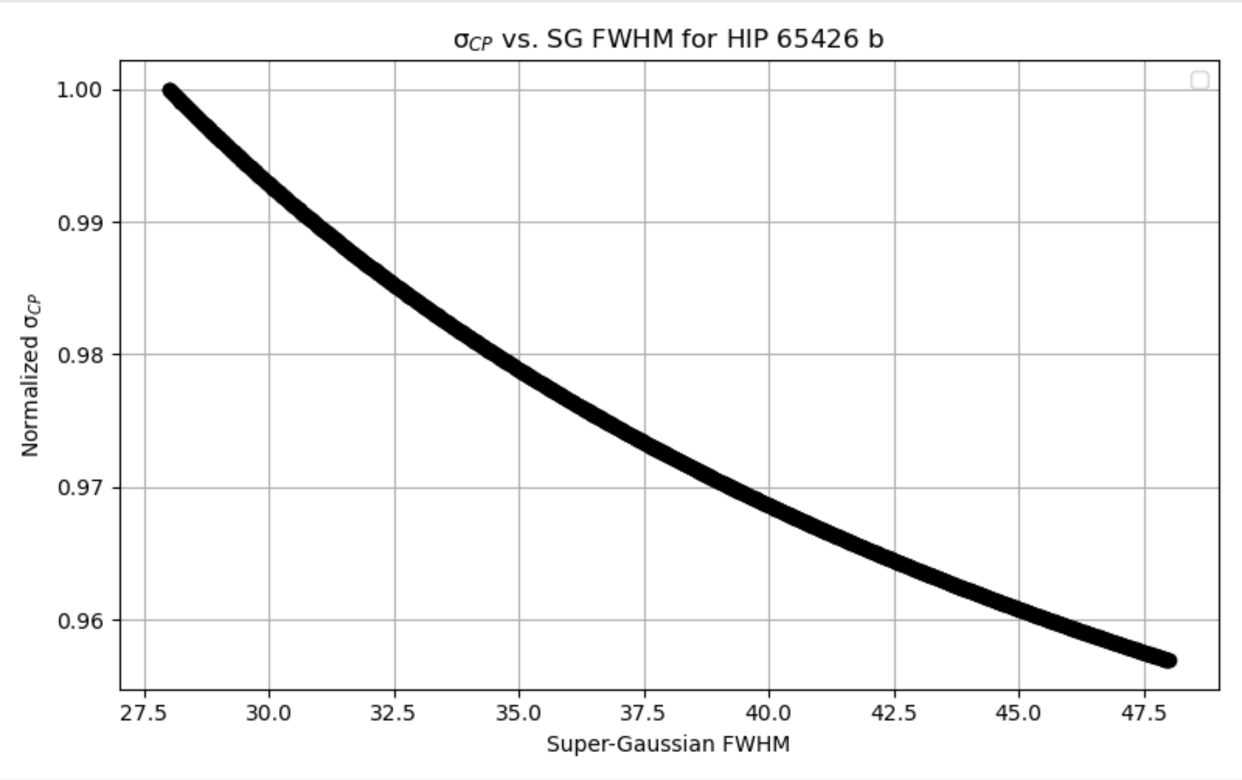

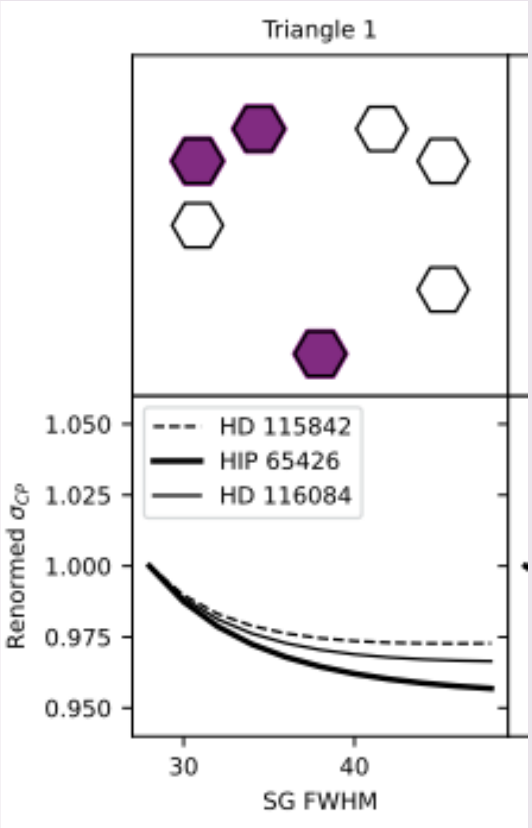

Credit: Sallum et al. 2024

1st Order Calculations

My 1st order calculations will be using exoplanet HIP 65426:

- Separation: 0.11 λ/D [17]
- Contrast: 7.6 Mag [17]
- Position Angle: 288.0° [17]
- **Assuming these values to use a Planet Injection Model

- Full Width at Half Maximum (FWHM) ~ 28-48 pixels [13]
- Telescope Diameter: 6.5 m [12]
- STD of Pixels: $\sigma_{pixel} = 100\ e^{-}$ [13]
- Wavelength of Filter used: $\lambda = 3.8\ \mu m$ [13]
- Number of Aperture Holes: 7 [13]

HIP 65426

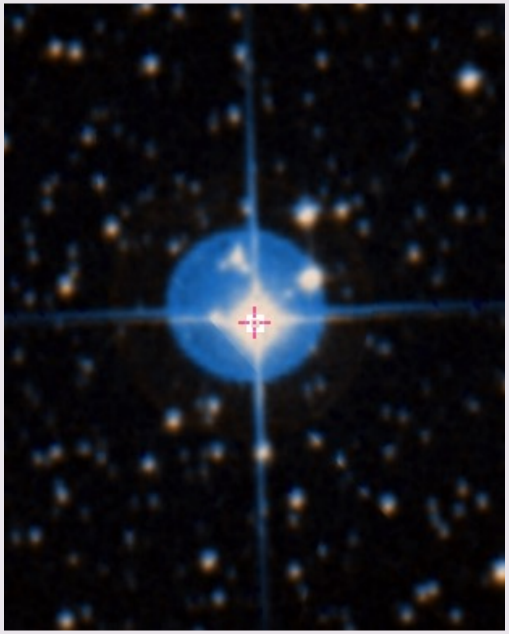

Credit: MAST

1st Order Calculations

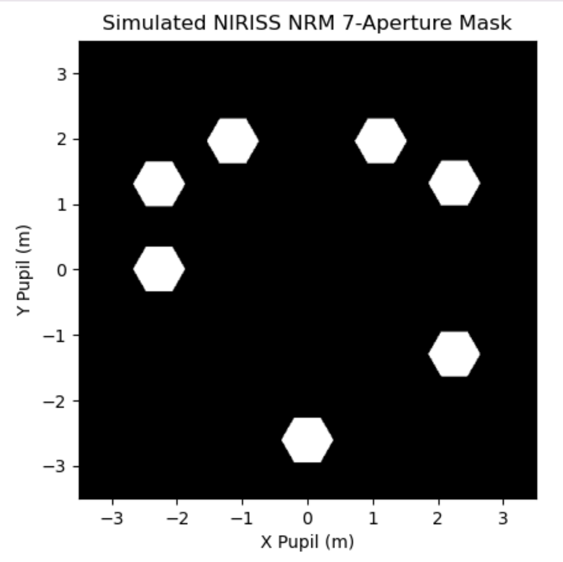

Credit: [Artigau et al. 2014]

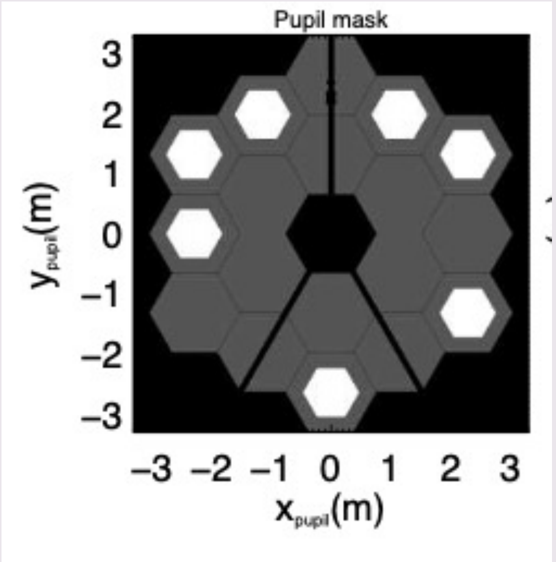

Credit: [Greenbaum et al. 2014]

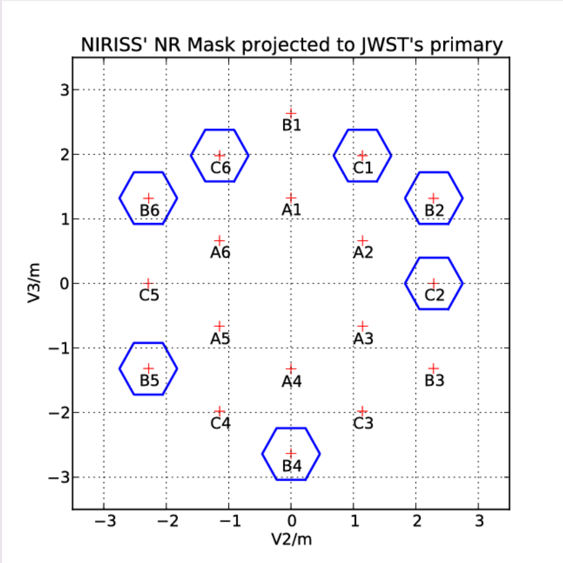

Hexagon Center Coordinates: B4 = [0, 2.6138], C2 = [-2.27365, 0],
B2 = [-2.27365, -1.30028], C1 = [-1.1427, -1.9574],
C6 = [1.1275, -1.9574], B6 = [2.2550,-1.3127],
B5 = [2.2531,1.2995] (m) [18]

1st Order Calculations

Hexagon Geometry:
Size = 0.8/2 (m) [17]
Hexagon Center coordinates: x0, y0 (m)
Where to place it on the grid: XI – x0, ETA-y0
Position Conditions:

$|XI - x| <= Size$

$|ETA - y0| <= \sqrt{3} * \frac{\text{Size}}{2}$

$\sqrt{3} * (|XI - x| + |ETA - y0|) <= \sqrt{3} * Size$

This will make the Aperture mask, P.

Point Spread Function: $F = |\mathcal{F}(P)|^2$

Logarithmic Intensity: $\log(I) = \log(\max(F, 1e - 12))$

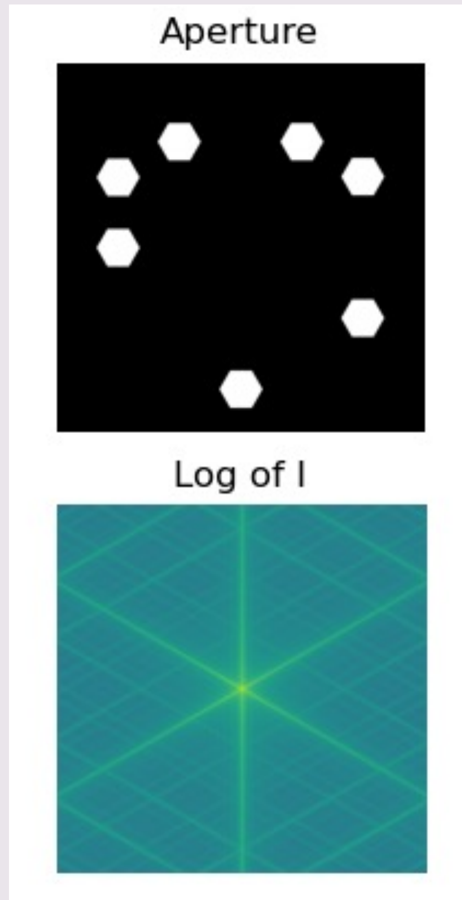

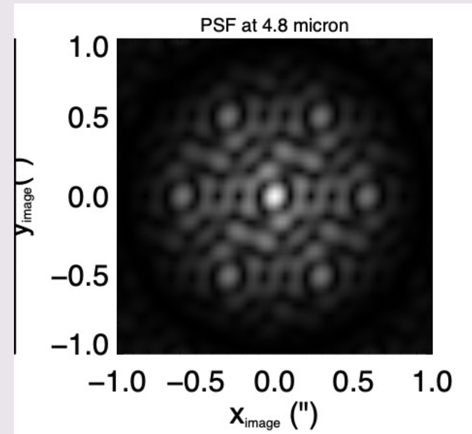

Credit: Artigau et al. 2014

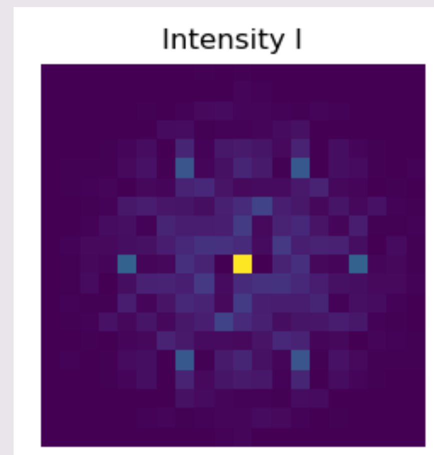

1^{st} Order Calculations

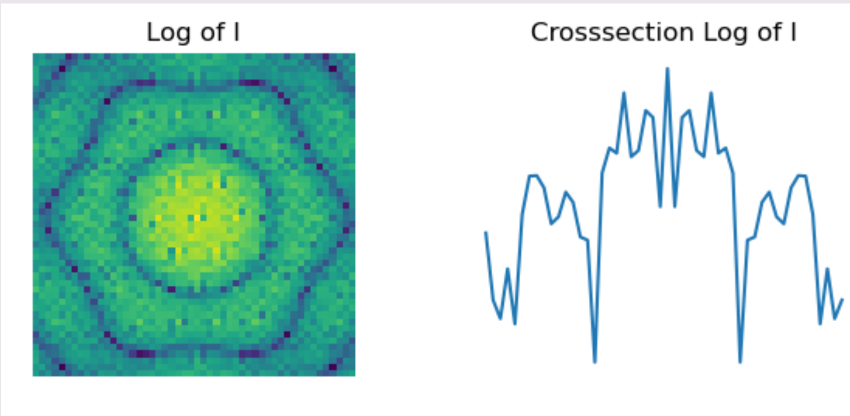

Logarithmic Intensity: $\log(I) = \log(\max(F, 1e - 12)$

Window Size: w = 25, w = very big (m)

When w is very large, we can see the behavior of the fringes. In literature they refer to them as square fringes. We can see these in the bottom right corner.

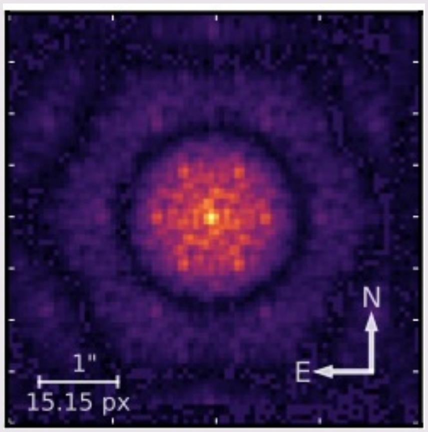

Credit: [Ray et al. 2025]

When w is 25 we can increase the size of the fringes, which more accurately represents what is found in literature.

The image from literature is a raw image of HIP 65426 created from the interference of light from AMI.

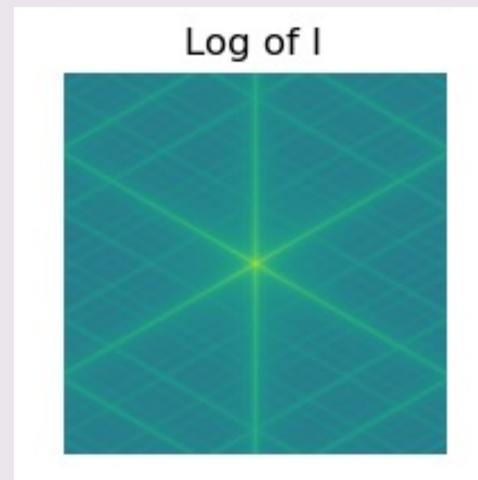

1st Order Calculations

Credit: [Sallum et al. 2024]

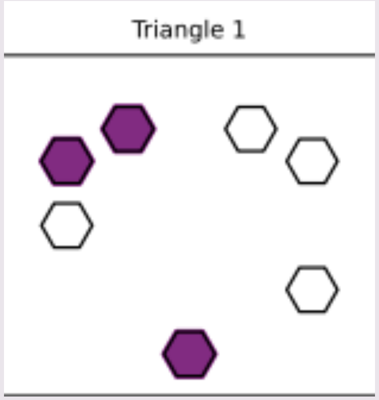

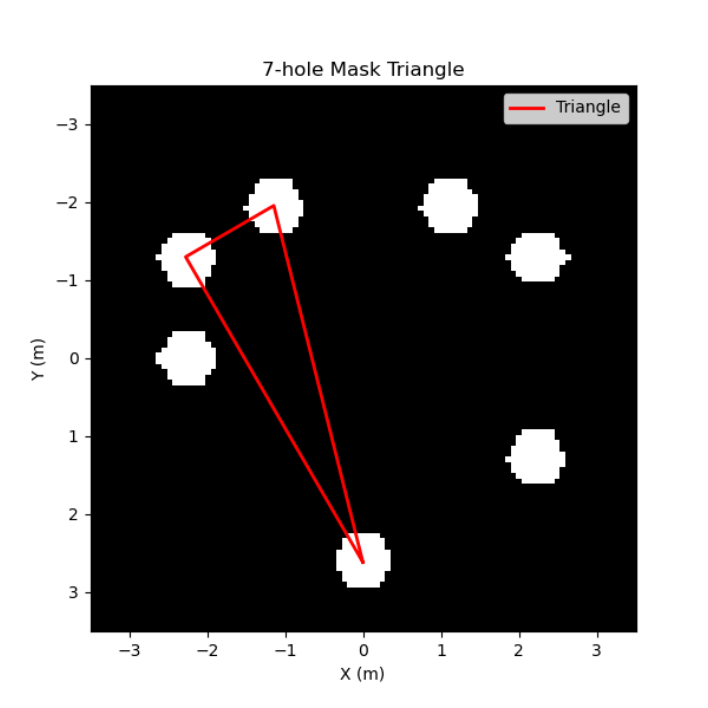

Baseline Vector: $b_{mn} = Center_n - Center_m$

Spatial Frequency Vector: $(u, v) = b_{mn}/\lambda$ [16]

Frequency Resolution: $fs = \frac{1}{N*dx}$

dx = 0.01 m

N = xi(max)-xi(min) $\approx$ 7 m

*Where xi is -3.5x3.5 m

Pixel Values: $(u_{idx}, v_{idx}) = \frac{(u,v)}{fs+N/2}$

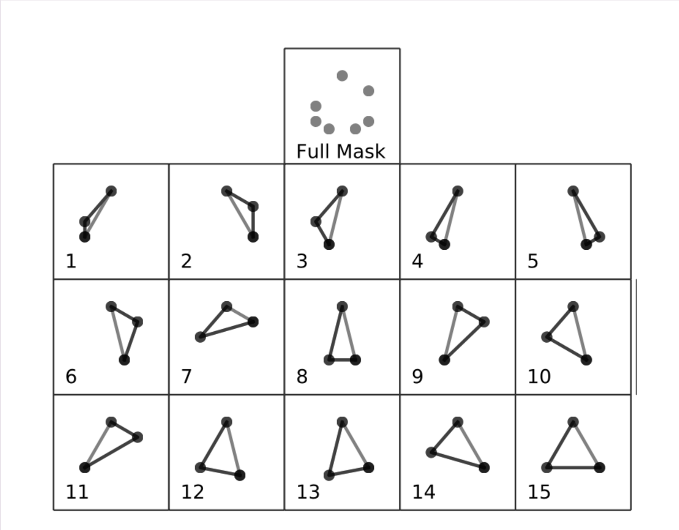

Credit: [Greenbaum et al. 2014]

1st Order Calculations

Squared Fringe Visibility: $V_{mn} = F[(u_{idx}, v_{idx})] \rightarrow real(a_{mn}) + imaginary(b_{mn})$ [8]

Fringe Phase: $\Delta\phi_{mn} = \arctan 2(b_{mn}, a_{mn})$ [16]

Closure Phase: $CP_m = V_{mn} e^{i\Delta\phi_{mn}}$ [8]

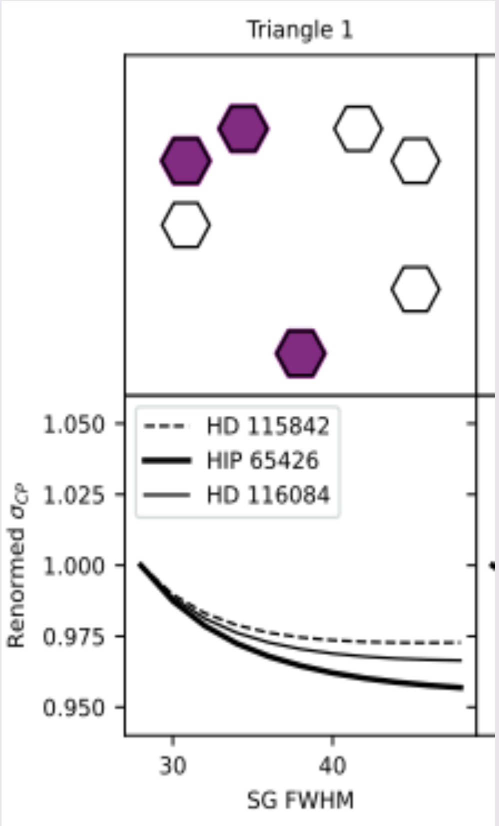

Credit: Sallum et al. 2024

1st Order Calculations

Closure Phase Standard Deviation: $\sigma_{cp} = \sqrt{0.5(N_{photons} + n_{pixel} * \sigma_{pixel}} \frac{N_{holes}}{N_{Photons}}$ [13]

Detected Photons: $N_{photons} = \sum F * SG$

# of Image Pixels weighted by SG: $n_{pixel} = \sum P * SG$

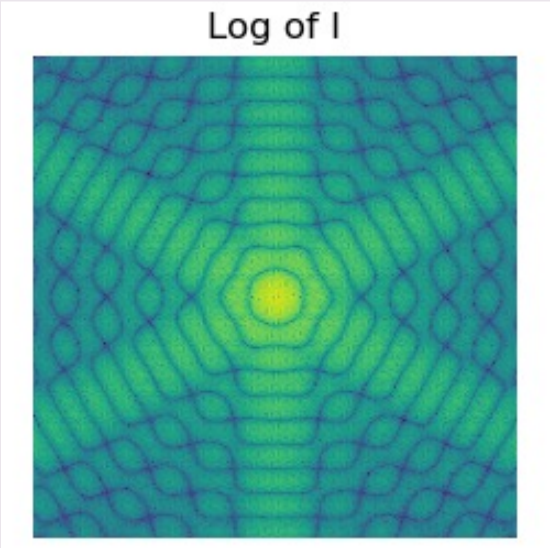

1^{st} Order Calculations

Super Gaussian Windowing: $SG = \exp^{-\frac{r^4}{\sigma}}$ [13]

Center Position of the Full Aperture: $r = \sqrt{x_{pix}^2 + y_{pix}^2}$

Standard Deviation of FWHM: $\sigma = \frac{FWHM}{(2ln2)^{\frac{1}{4}}}$ [13]

1st Order Calculations

Renormalized σ_{cp} : $Normed\ \sigma_{cp} = \frac{\sigma_{cp}}{\sigma_{cp}(@\ FWHM=28)}$

FWHM = 28 pixels - 48 Pixels [13]

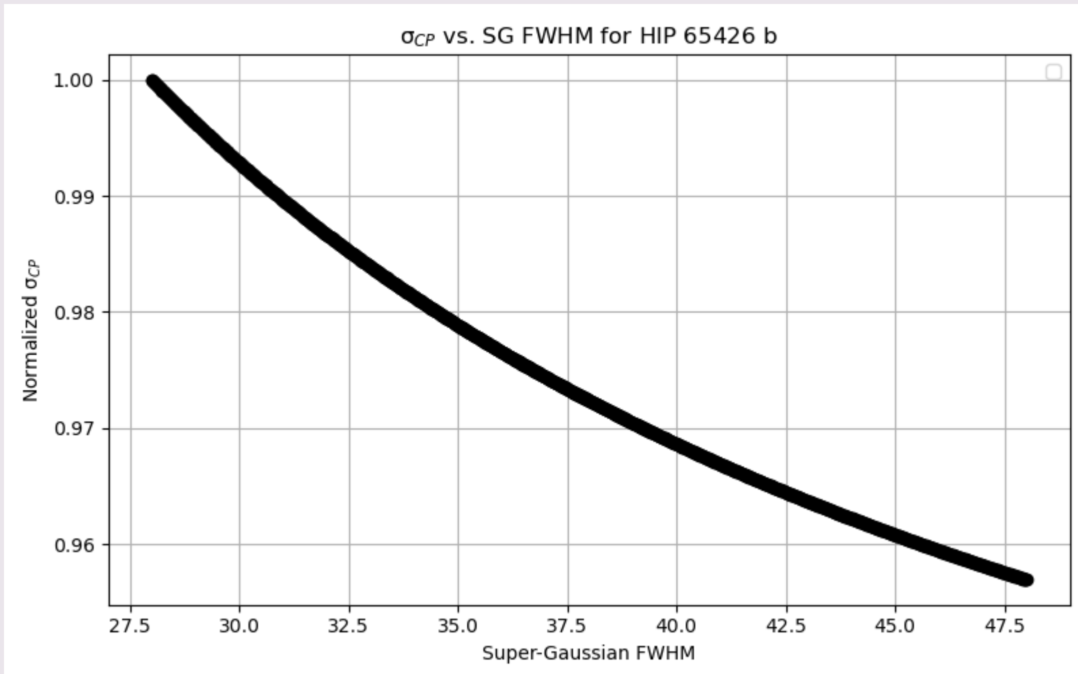

Comparison

- FWHM = 28 Pixels:
  - Simulated = 1.00
  - Literature ≈ 1.00 [13]
- FWHM = 48 Pixels:
  - Simulated = 0.9569
  - Literature ≈ 0.960 [13]

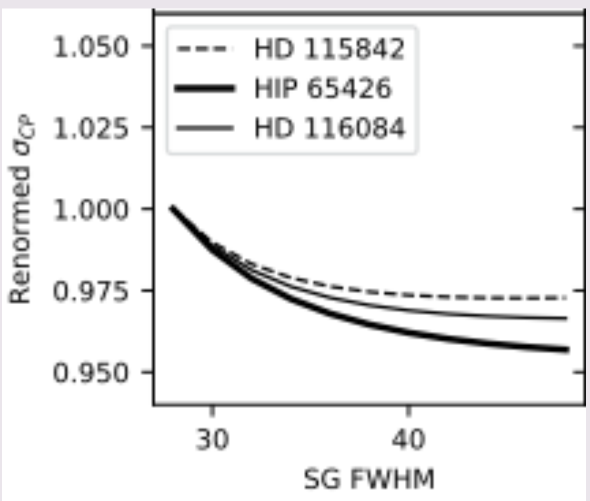

Credit: [Sallum et al. 2024]

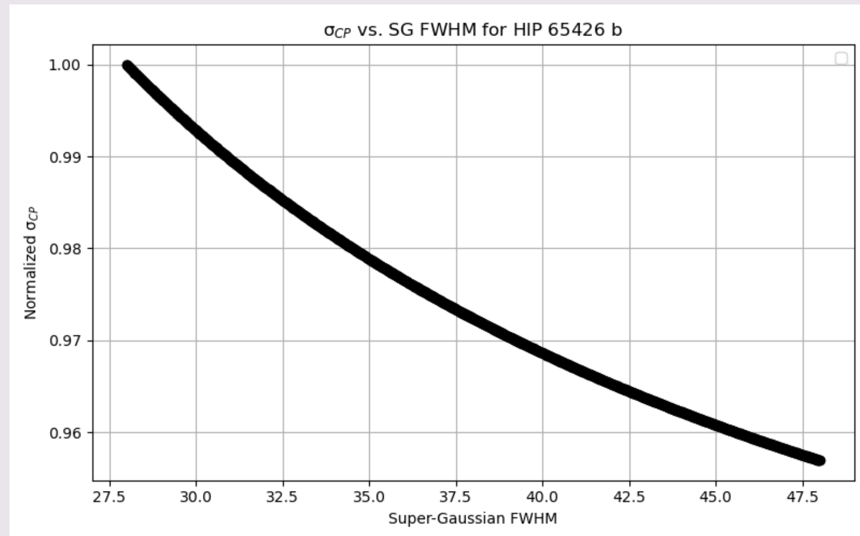

% Error: $E = \frac{|Simulated - Literature|}{Literature} * 100 = 0.3\%$

Iterated 1000 times

Summary

- Created a PSF based on the NIRISS AMI 7 hole NRM
- Applied Super Gaussian apodization
- Modeled the Closure Phase Renormalized Standard Deviation around the mean and compared it to the FWHM after literature
- Modeled the square fringes the AMI produces

Credit: Sivaramakrishnan et al. 2023

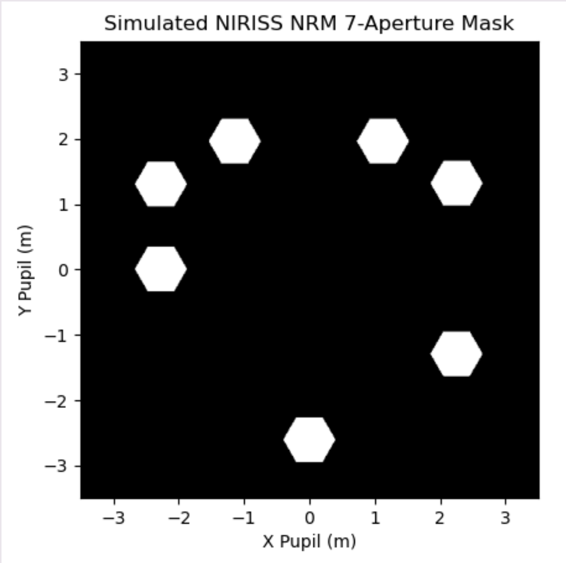

Questions?

References

[1] Anand Sivaramakrishnan, Peter Tuthill, James P. Lloyd, Alexandra Z. Greenbaum, Rachel A. Cooper, Thomas Vandal, Jens Kammerer, Joel Sanchez-Bermudez, Benjamin J. S. Pope, Dori Blakely, Lo ïc Albert, Neil J. Cook, Doug Johnstone, Andre R. Martel, Kevin Volk, Anthony Soulain, K. E. Saavik Ford, Barry McKernan, M. Begon ã Vila, Neil Rowlands, Rene Doyon, Louis Desdoigts, Alexander W. Fullerton, Matthew De Furio, Paul Goudfrooij, Sherie T. Holfeltz, Stephanie LaMassa, Michael Maszkiewicz, Michael R. Meyer, Marshall D. Perrin, Laurent Pueyo, Johannes Sahlmann, Sangmo Tony Sohn, Paula S. Teixeira, 2022. The Near Infrared Imager and Slitless Spectrograph for the James Webb Space Telescope - IV. Aperture Masking Interferometry. https://arxiv.org/pdf/2210.17434.

[2] Adam B. Langeveld , Aleks Scholz , Koraljka Mu ˇzic ́, Ray Jayawardhana , Daniel Capela , Lo ïc Albert , Rene Doyon , Laura Flagg , Matthew de Furio , Doug Johnstone, David Lafre`niere , Michael Meyer, 2024. The JWST/NIRISS Deep Spectroscopic Survey for Young Brown Dwarfs and Free-Floating Planets. https://arxiv.org/pdf/2408.12639.

[3] Information@eso.org. (n.d.). *Peeking into perseus*. www.esawebb.org. https://esawebb.org/images/potm2408a/.

[4] Atmosphere composition of exoplanet K2-18 b (Niriss & NIRSpec) | Webb. (n.d.). https://webbtelescope.org/contents/media/images/2023/139/01H9RF0CCN4MZYDG56O7K33WQV.

[5] *JWST User Documentation*. JWST Near Infrared Imager and Slitless Spectrograph - JWST User Documentation. (n.d.). https://jwst-docs.stsci.edu/jwst-near-infrared-imager-and-slitless-spectrograph#gsc.tab=0.

[6] Cesari, T. (2022, June 3). *The modes of Webb's niriss*. NASA. https://blogs.nasa.gov/webb/2022/06/03/the-modes-of-webbs-niriss/.

https://jwst-docs.stsci.edu/jwst-near-infrared-imager-and-slitless-spectrograph/niriss-observing-strategies/niriss-ami-recommended-strategies#gsc.tab=0

[8] Anand Sivaramakrishnan, Peter Tuthill, James P. Lloyd, Alexandra Z. Greenbaum, Deepashri Thatte, Rachel A. Cooper, Thomas Vandal, Jens Kammerer, Joel Sanchez-Bermudez, Benjamin J. S. Pope, Dori Blakely, Lo ïc Albert, Neil J. Cook, Doug Johnstone, Andre R. Martel, Kevin Volk, Anthony Soulain, K. E. Saavik Ford, Etienne Artigau, David Lafrenie`re, Chris J. Willott, Se ́bastien Parmentier McKernan, M. Begon ã Vila, Neil Rowlands, Rene Doyon, Louis Desdoigts, Alexander W. Fullerton, Matthew De Furio, Paul Goudfrooij, Sherie T. Holfeltz, Stephanie LaMassa, Michael Maszkiewicz, Michael R. Meyer, Marshall D. Perrin, Laurent Pueyo, Johannes Sahlmann, Sangmo Tony Sohn, and Paula S. Teixeira. 2024. The Near Infrared Imager and Slitless Spectrograph for the James Webb Space Telescope - IV. Aperture Masking Interferometry. https://www.researchgate.net/publication/368394197_The_Near_Infrared_Imager_and_Slitless_Spectrograph_for_the_James_Webb_Space_Telescope_IV_Aperture_Masking_Interferometry .

[9] Webb's science tools | Webb. (n.d.-b). https://webbtelescope.org/contents/articles/whats-in-webbs-toolkit.

[10] *L09: Signal-to-noise ratios: Phy241*. L09: Signal-to-Noise ratios | PHY241. (n.d.). https://sheffield-mps.github.io/PHY241/lectures/l09/.

[11] Doyon, Rene ́, Chris J. Willott , John B. Hutchings, Anand Sivaramakrishnan , Lo ïc Albert , David Lafrenie`re , Neil Rowlands , M. Begon ã Vila , Andre R. Martel, Stephanie LaMassa , David Aldridge, Etienne Artigau , Peter Cameron, Pierre Chayer , Neil J. Cook , Rachel A. Cooper , Antoine Darveau-Bernier , Jean Dupuis, Colin Earnshaw, Ne ́stor Espinoza , Joseph C. Filippazzo , Alexander W. Fullerton , Daniel Gaudreau, Roman Gawlik, Paul Goudfrooij , Craig Haley, Jens Kammerer , David Kendall, Scott D. Lambros, Luminita Ilinca Ignat, Michael Maszkiewicz, Ashley McColgan, Takahiro Morishita , Nathalie N.-Q. Ouellette , Camilla Pacifici , Natasha Philippi, Michael Radica , Swara Ravindranath , Jason Rowe , Arpita Roy , Karl Saad, Sangmo Tony Sohn , Geert Jan Talens , Deepashri Thatte, Joanna M. Taylor , Thomas Vandal , Kevin Volk , Michel Wander, Gerald Warner, Sheng-Hai Zheng, Julia Zhou, Roberto Abraham , Mathilde Beaulieu, Bjo ̈rn Benneke, Laura Ferrarese , Ray Jayawardhana , Doug Johnstone , Lisa Kaltenegger , Michael R. Meyer , Judy L. Pipher , Julien Rameau , Marcia Rieke , Salma Salhi , Marcin Sawicki, 2023. The Near Infrared Imager and Slitless Spectrograph for the James Webb Space Telescope - I. Instrument Overview and in-Flight Performance. https://arxiv.org/pdf/2306.03277.

[12] Michael Maszkiewicz, 2012. *Near- Infrared Imager and Slitless Spectrograph (NIRISS): a new instrument on James Webb Space Telescope (JWST).* *https://www.spiedigitallibrary.org/conference-proceedings-of-spie/10564/2309161/Near--infrared-imager-and-slitless-spectrograph-NIRISS--a/10.1117/12.2309161.full*.

[13] Sallum, S., Ray, S., Kammerer, J., Sivaramakrishnan, A., Cooper, R., Greebaum, A. Z., ... Zurlo, A. (2024). *The JWST early release science program for direct observations of exoplanetary systems: IV. NIRISS aperture masking interferometry performance and lessons learned. Astrophysical Journal Letters, 963*(1), L2. doi:10.3847/2041-8213/ad21fb

[14] Greenbaum, Alexandra & Pueyo, Laurent & Sivaramakrishnan, Anand & Lacour, Sylvestre. (2014). *An Image-plane Algorithm for JWST's Non-redundant Aperture Mask Data. The Astrophysical Journal*. 798. 10.1088/0004-637X/798/2/68.

[15] Artigau, Étienne & Sivaramakrishnan, Anand & Greenbaum, Alexandra & Doyon, Rene & Goudfrooij, Paul & Fullerton, Alex & Lafrenière, David & Volk, Kevin & Albert, Loïc & Martel, André & Ford, K. & McKernan, Barry. (2014). *NIRISS aperture masking interferometry: An overview of science opportunities. Proceedings of SPIE - The International Society for Optical Engineering*. 9143. 10.1117/12.2055191.

[16] Soulain, Anthony & Sivaramakrishnan, Anand & Tuthill, Peter G. & Thatte, Deepashri & Volk, Kevin & Cooper, Rachel & Albert, Loïc & Artigau, Étienne & Cook, Neil & Doyon, René & Johnstone, Doug & Lafrenière, David & Martel, André R. (2022). *The James Webb Space Telescope aperture masking interferometer*, https://arxiv.org/pdf/2201.01524.

References Cont.

[17] Shrishmoy Ray and Steph Sallum and Sasha Hinkley and Anand Sivamarakrishnan and Rachel Cooper and Jens Kammerer and Alexandra Z. Greebaum and Deepashri Thatte and Tomas Stolker and Cecilia Lazzoni and Andrei Tokovinin and Matthew de Furio and Samuel Factor and Michael Meyer and Jordan M. Stone and Aarynn Carter and Beth Biller and Andrew Skemer and Genaro Suarez and Jarron M. Leisenring and Marshall D. Perrin and Adam L. Kraus and Olivier Absil and William O. Balmer and Mickael Bonnefoy and Marta L. Bryan and Sarah K. Betti and Anthony Boccaletti and Mariangela Bonavita and Mark Booth and Brendan P. Bowler and Zackery W. Briesemeister and Faustine Cantalloube and Gael Chauvin and Valentin Christiaens and Gabriele Cugno and Thayne Currie and Camilla Danielski and Trent J. Dupuy and Jacqueline K. Faherty and Christine H. Chen and Per Calissendorff and Elodie Choquet and Michael P. Fitzgerald and Jonathan J. Fortney and Kyle Franson and Julien H. Girard and Carol A. Grady and Eileen C. Gonzales and Thomas Henning and Dean C. Hines and Kielan K. W. Hoch and Callie E. Hood and Alex R. Howe and Markus Janson and Paul Kalas and Grant M. Kennedy and Matthew A. Kenworthy and Pierre Kervella and Daniel Kitzmann and Masayuki Kuzuhara and Anne-Marie Lagrange and Pierre-Olivier Lagage and Kellen Lawson and Ben W. P. Lew and Michael C. Liu and Pengyu Liu and Jorge Llop-Sayson and James P. Lloyd and Anna Lueber and Bruce Macintosh and Elena Manjavacas and Sebastian Marino and Mark S. Marley and Christian Marois and Raquel A. Martinez and Brenda C. Matthews and Elisabeth C. Matthews and Dimitri Mawet and Johan Mazoyer and Michael W. McElwain and Stanimir Metchev and Brittany E. Miles and Maxwell A. Millar-Blanchaer and Paul Molliere and Sarah E. Moran and Caroline V. Morley and Sagnick Mukherjee and Paulina Palma-Bifani and Eric Pantin and Polychronis Patapis and Simon Petrus and Laurent Pueyo and Sascha P. Quanz and Andreas Quirrenbach and Isabel Rebollido and Jea Adams Redai and Bin B. Ren and Emily Rickman and Matthias Samland and B. A. Sargent and Joshua E. Schlieder and Glenn Schneider and Karl R. Stapelfeldt and Ben J. Sutlieff and Motohide Tamura and Xianyu Tan and Christopher A. Theissen and Taichi Uyama and Arthur Vigan and Malavika Vasist and Johanna M. Vos and Kevin Wagner and Jason J. Wang and Kimberly Ward-Duong and Niall Whiteford and Schuyler G. Wolff and Kadin Worthen and Mark C. Wyatt and Marie Ygouf and Xi Zhang and Keming Zhang and Zhoujian Zhang and Yifan Zhou.(2025*). The JWST Early Release Science Program for Direct Observations of Exoplanetary Systems III: Aperture Masking Interferometric Observations of the star HIP 65426 at 3.8 um,* https://arxiv.org/pdf/2310.11508.

[18] JWST ERS-1386 Team. (n.d.). *NIRISS_7holeMask.txt*. GitHub. https://github.com/JWST-ERS1386-AMI/SAMpy/blob/main/NIRISS_7holeMask.txt

Code Appendix:

```
import matplotlib.pyplot as plt
import numpy as np
from astropy.io import fits
import amical
from amical import fits2obs
import os

def prop(A):
   return np.abs(np.fft.fftshift(np.fft.fftn(A)))

def makefig(P, w=128):
   plt.figure()
   F = prop(P)**2
   logf = np.log(np.maximum(F, 1e-12))  # avoid log(0) issues
   W = P.shape[0]//2
   N = P.shape[0]
   freq = np.fft.fftshift(np.fft.fftfreq(N, d=1))
   U, V = np.meshgrid(freq, freq)
   plt.subplot(221)
   plt.title("Aperture")
   W = P.shape[0]//2
   plt.imshow(np.real(P)[W-w:W+w,W-w:W+w])
   plt.subplot(222)
   plt.title("Intensity I")
   plt.imshow(F[W-w:W+w, W-w:W+w])
   plt.axis("off")
   plt.subplot(223)
   plt.title("Log of I")
   plt.imshow(logf[W-w:W+w, W-w:W+w])
   plt.axis("off")
   plt.subplot(224)
   plt.title("Crosssection Log of I")
   plt.plot(logf[W, W-w:W+w])
   plt.axis("off")
```

```
def add_hexagonal_aperture(XI, ETA, centers, size):
   P = np.zeros_like(XI)
   sqrt3 = np.sqrt(3)
   for x0, y0 in centers:
      x = XI - x0
      y = ETA - y0
      mask = (np.abs(x) <= size) & \
           (np.abs(y) <= sqrt3 * size / 2) & \
           (sqrt3 * np.abs(x) + np.abs(y) <= sqrt3 * size)
      P += mask.astype(float)
   return P

def SG(XI, ETA, fwhm, n=4):
   S_Gaus = np.zeros(XI.shape)
   n_p = np.zeros(fwhm.shape)
   for i in range(len(fwhm)):
      R = np.sqrt(XI**2 + ETA**2)
      sig = fwhm[i]/((2*np.log(2))**(1/n))
      S_Gaus = np.exp(-(R / sig)**n)
      n_p[i] = np.sum(S_Gaus)
   return S_Gaus, n_p
```

```
def trig_Angles(C1, C2, C3, P, xi):
   N = xi.max()-xi.min()
   print(N)
   dx= 0.01
   fs = 1/(N*dx)
   #taking the pupil plane coordinates in meters to find the baselines
   BL12 = C2-C1
   BL23 = C3-C2
   BL31 = C1-C3
   F = np.fft.fftshift(np.fft.fftn(P))

   Bmean = (np.linalg.norm(BL12)+np.linalg.norm(BL23)+np.linalg.norm(BL31))/3
   #Need to pick a new value for lamda
   lamda = 3.8

   #computing the spatial frequency vector
   (u1, v1) = BL12/lamda
   (u2, v2) = BL23/lamda
   (u3, v3) = BL31/lamda
   mag1 = np.sqrt(u1**2 + v1**2)
   mag2 = np.sqrt(u2**2 + v2**2)
   mag3 = np.sqrt(u3**2 + v3**2)
   f = (mag1+mag2+mag3)/3

   u1_idx = int(np.round(u1 / fs + N / 2))
   v1_idx = int(np.round(v1 / fs + N / 2))
   u2_idx = int(np.round(u2 / fs + N / 2))
   v2_idx = int(np.round(v2 / fs + N / 2))
   u3_idx = int(np.round(u3 / fs + N / 2))
   v3_idx = int(np.round(v3 / fs + N / 2))
   print(u1_idx)

   V1_mn = F[v1_idx, u1_idx]

   a1 = np.real(V1_mn)
   b1 = np.imag(V1_mn)
   V2_mn = F[v2_idx, u2_idx]
   a2 = np.real(V2_mn)
   b2 = np.imag(V2_mn)
   V3_mn = F[v3_idx, u3_idx]
   a3 = np.real(V3_mn)
   b3 = np.imag(V3_mn)

   vis_amps = np.array(([np.abs(V1_mn)],[np.abs(V2_mn)],[np.abs(V3_mn)]))
   vis_phases = np.array(([np.angle(V1_mn)], [np.angle(V2_mn)], [np.angle(V3_mn)]))
```

```
   V = np.vstack(([V1_mn], [V2_mn], [V3_mn]))
   b = np.vstack(([b1], [b2], [b3]))
   b2 = np.vstack(([np.linalg.norm(BL12)], [np.linalg.norm(BL23)], [np.linalg.norm(BL31)]))
   a = np.vstack(([a1], [a2], [a3]))
   print(f"B matrix: {b}")
   print(f"Transformation: {BL12}")
   phi1 = np.atan2(b[0],a[0])
   phi2 = np.atan2(b[1],a[1])
   phi3 = np.atan2(b[2],a[2])
   ClosurePhase = np.angle(np.exp(1j *(phi1 + phi2 + phi3)))
   return ClosurePhase, Bmean, b2, vis_amps, vis_phases, f
```

Rensselaer 1824 · 2024 200

Code Appendix Cont.

```
def plot_aperture_with_triangle(centers, triangle):
    plt.figure(figsize=(6, 6))
    plt.imshow(P, cmap='gray', extent=[-3.5, 3.5, 3.5, -3.5])
    x = centers[triangle, 0]
    y = centers[triangle, 1]
    plt.plot(np.append(x, x[0]), np.append(y, y[0]), 'r-', lw=2, label='Triangle')
    plt.title("7-hole Mask Triangle")
    plt.xlabel("X (m)"); plt.ylabel("Y (m)")
    plt.legend()
    plt.gca().set_aspect('equal')
    plt.show()

def inject_companion(P, sep, pa_deg, contrast):
    theta_rad = np.deg2rad(pa_deg)
    dx = sep * np.cos(theta_rad)
    dy = sep * np.sin(theta_rad)
    phase = 2 * np.pi * (XI * dx + ETA * dy)
    return P + contrast * P * np.exp(1j * phase)
```

```
#Grid setup in meters
N = 100
xi = np.linspace(-3.5, 3.5, N) #meters
XI, ETA = np.meshgrid(xi, xi)
N_holes = 7
Dia = 6.5 #m
# h = 6.626*(10**-34) #J*s
# c = 3*(10**8) #m/s
lamda = 3.8 #mum
sig = 5
fwhms = np.linspace(28, 48, 100)
# np = 2*(80*80)
sigpix = 100 #electrions^2 <- from JWST Documentation
XSqua = 25 #corresponds to sig = 5

#HIP 65426 Values pulled from literature
planet_sep = 0.11# in lambda/D units
planet_pa_deg = 288  # position angle in degrees (0 = along x-axis)
planet_contrast = 7.6 # flux ratio (mag ~ 6.5)

#Parameters for hexagon layout
size = 0.4  # hexagon half-width
L = 0.3     # spacing from center
centers = np.array(([0, 2.6138], [-2.27365, 0], [-2.27365, -1.30028], [-1.1427, -1.9574],[1.1275, -1.9574], [2.2550,-1.3127], [2.2531,1.2995]))
# B4, C2, B2, C1, C6, B6, B5

#Create combined aperture and plot
P = add_hexagonal_aperture(XI, ETA, centers, size)
makefig(P, w = 35)  #adjust zoom to fit all 7

#making the Super guassian
SG,n_pix = SG(XI, ETA, fwhms)
P = P/ np.sum(P)
SigCP = []
closure_angles = []
```

Code Appendix Cont.

```
for fwhm in fwhms:
   # Generate Super-Gaussian window for this FWHM
   sig = fwhm / ((2 * np.log(2)) ** (1 / 4))

   #Creating a Pixel grid
   N = 100
   yc, xc = N // 2, N // 2
   YY, XX = np.indices((N, N))
   R = np.sqrt((XX - xc)**2 + (YY - yc)**2)
   SG = np.exp(-(R / sig)**4)
   P = add_hexagonal_aperture(XI, ETA, centers, size)
   n_pix = np.sum(SG*P)

# Apply SG to PSF
   P_w = np.abs(prop(P))**2 * SG
   N_g = np.sum(P_w)
   P_inj = inject_companion(P_w, planet_sep, planet_pa_deg, planet_contrast)
   # (ClosurePhase1, Bmean1, b1, V1, Vp, f1) = trig_Angles(centers[0], centers[2] , centers[3], P_inj, xi)
   # closure_angles.append(np.rad2deg(ClosurePhase1))  # convert to degrees if needed

   # Compute sigma_CP
   #both of these sigmas are from literature, but the uncommented one accounts for more noise
   #sig_cp = (N_holes / N_pho) * np.sqrt(1.5)
   sig_cp = (N_holes / N_g) * np.sqrt(0.5 * (N_g+ n_pix * sigpix))
   SigCP.append(sig_cp)

SigCP = np.array(SigCP)
```

```
# Normalizing, and then printing the associated values
SigCP_renorm = SigCP / SigCP[0]
print("FWHM (px)   Normalized σ_CP")
for i in range(len(fwhms)):
   print(f"{fwhms[i]:>8}  {SigCP_renorm[i]:.4f}")

plt.figure(figsize=(8, 5))
plt.plot(fwhms, SigCP_renorm, 'o-k')
plt.xlabel("Super-Gaussian FWHM")
plt.ylabel("Normalized σ$_{CP}$")
plt.title("σ$_{CP}$ vs. SG FWHM for HIP 65426 b")
plt.legend()
plt.grid(True)
plt.tight_layout()
plt.show()
plot_aperture_with_triangle(centers, [0, 2, 3])  # B4, B2, C1

#Finding the values of the thre triangles used in the referenced literature
#Using Triangle 1, B4, B2, C1
(ClosurePhase1, Bmean1, b1, V1, Vp, f1) = trig_Angles(centers[0], centers[2] , centers[3], P_inj, xi)

#Using Triangle 2, C2, C6, C1
ClosurePhase2, Bmean2, b2, V2 ,Vp2, f2 = trig_Angles(centers[1], centers[3] , centers[4], P_inj, xi)

#Using Triangle 3, C2, B2, B6
ClosurePhase3, Bmean3, b3, V3 , Vp3, f3= trig_Angles(centers[1], centers[2] , centers[5], P_inj, xi)
```